

Collaborative Self-Perception Network Architecture for Hyperspectral Image Change Detection

Jiao Shi¹, Zeping Zhang, Tiancheng Wu, Xi Zhang, and Yu Lei²

Abstract—Despite the great advantages in deep feature representation when dealing with change detection (CD) problem, the designs of neural networks were time-consuming processes of trial and error. In addition, the traditional CD methods based on deep neural networks (DNN) only deal with one dataset at a time, which has limited learning knowledge and undoubtedly fails to take advantage of the common characteristics among similar datasets. For hyperspectral images (HSIs) obtained by the same sensor, the spectral information has a similar physical meaning (radiance or reflectivity). To utilize the inherent similarity within hyperspectra for learning a robust difference signature, a collaborative analysis framework with self-perception network architecture (SPNA-CA) is proposed to efficiently learn from multiple datasets and leverage their synergy. Different network architecture searching tasks are established for each dataset pertinently, in which the evolutionary multitasking self-perception network architecture (SPNA) method is designed for exploring effective and reasonable network architectures. Besides, a cross-task knowledge transfer mechanism (CKTM) is proposed to transfer excellent network architecture information, which improves the efficiency of the collaborative analysis framework. Experimental results confirm the effectiveness of collaborative analysis for solving HSI-CD problems among multiple datasets.

Index Terms—Change detection (CD), deep neural networks (DNNs), evolutionary multitasking optimization, hyperspectral images (HSIs).

I. INTRODUCTION

IMAGE change detection (CD) is an important application of remote sensing to identify the desired significant changes between bitemporal images. CD is applied to diverse applications, such as land cover mapping [1], disaster assessment [2], and sprawl analysis [3]. Hyperspectral images (HSI) with high spectral resolution and more bands can provide richer information than other remote sensing images [4], which has arisen lots of research [5], [6]. Furthermore, the high feature dimensionality and spectral interference of HSI data make the HSI-CD a challenging problem to solve with.

So far, scholars have already carried out some research on HSI-CD. Traditional CD methods, such as iteratively reweighted multivariate alteration detection (IR-MAD) [7], temporal-principal component analysis (TPCA) [8], and

change vector analysis (CVA) [9], provide some reliable measures of correlation in changes. However, those methods compress the high-dimensional spectrum variations into one or few dimensions, which may result in limited capability in excavating all the features of change.

Deep networks have powerful capabilities in modeling the spatial relationship between image object and its real-world geographical features, which can tackle high-dimensional data. Du *et al.* [10] proposed a CD method based on deep network and slow feature analysis (DSFA) theory, which shows that image transformation could effectively highlight the changed information. To better handle the high-dimensional problem of HSI data, a general end-to-end 2-D convolutional neural network (CNN) (GETNET) framework is proposed for HSI-CD [11]. Saha *et al.* [12] proposed a CD method using an untrained model and further comparing the extracted features using Deep CVA. In [13], a manifold-based method is proposed for dimensionality reduction to realize HSI-CD.

However, these methods only perform one CD task by analyzing one specific dataset at a time and start the CD task from the zero ground state of knowledge, which cannot effectively mine useful information among different datasets, while for HSIs obtained by the same sensor, the spectral information has similar physical meaning (radiance or reflectivity), which is independent of the dataset [14], [15]. Therefore, there is the possibility of knowledge sharing between different datasets of the same sensor. Moreover, traditional networks for CD are typically designed by human experts, which is time-consuming. Especially when dealing with multiple datasets, they have to design networks independently and repeatedly, making it more monotonous. In our previous work [16], a self-adaptive network was proposed to generate better network architectures for CD of a synthetic aperture radar (SAR) image, which effectively solves the problem of fixed structure. The network-generating method is exceedingly expected to be applied in multiple CD tasks to learn knowledge between similar but different datasets. In summary, it is worth studying how to establish the relationship among multiple datasets and effectively share knowledge to search better network architectures for HSI-CD.

A collaborative analysis framework with self-perception network architecture (SPNA-CA) is proposed to solve HSI-CD problems. In this letter, four contributions are highlighted.

- 1) A collaborative analysis framework (CA) is proposed to leverage potential correlations among multiple datasets, which models each CD task jointly with other related

Manuscript received October 2, 2021; revised November 21, 2021; accepted December 7, 2021. Date of publication March 8, 2022; date of current version March 29, 2022. This work was supported by the National Natural Science Foundation of China under Grant 62076204 and Grant 61806166. (Corresponding author: Yu Lei.)

The authors are with the School of Electronics and Information, Northwestern Polytechnical University, Xi'an 710072, China (e-mail: lei@nwpu.edu.cn).

Digital Object Identifier 10.1109/LGRS.2022.3157916

1558-0571 © 2022 IEEE. Personal use is permitted, but republication/redistribution requires IEEE permission.
See <https://www.ieee.org/publications/rights/index.html> for more information.

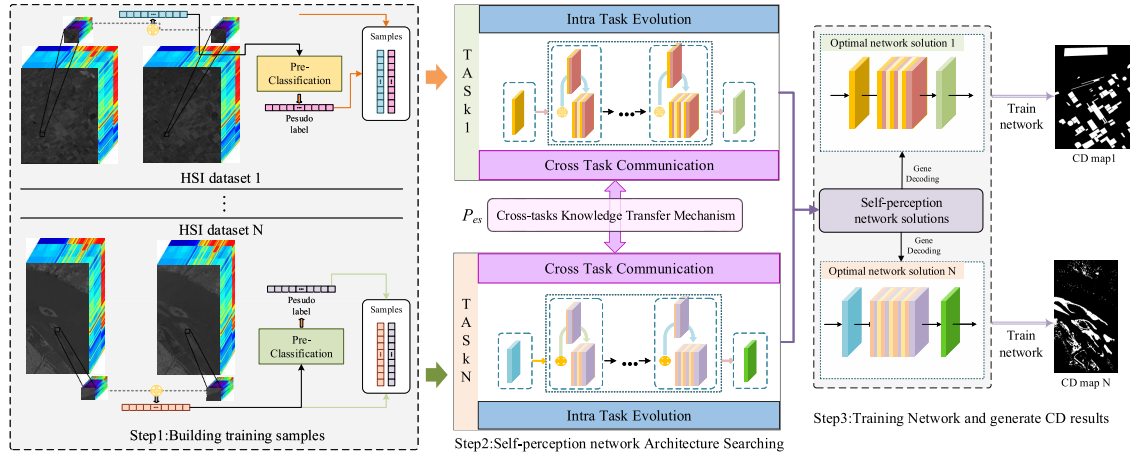


Fig. 1. Flowchart of the proposed HSI-CD method with SPNA-CA.

tasks to facilitate the flow of information by sharing knowledge.

- 2) Self-perception network architecture (SPNA) based on evolutionary multitasking optimization is proposed to lead the architecture generation, thereby giving rise to some effective and suitable networks associating with multiple datasets.
- 3) A cross-task knowledge transfer mechanism (CKTM) is proposed to transfer excellent network architecture information among SPNA tasks, which improves the cooperation ability of CA framework and strengthens the searching efficiency.
- 4) Considering the detection performance and network complexity, a hybrid-criteria selection strategy is designed for discovering high-quality yet simple network architectures.

In the following, Section II details the proposed method. Sections III and V show related experiments and analysis. Finally, Section IV gives a final conclusion on the proposed method.

II. METHODOLOGY

As shown in Fig. 1, the proposed SPNA-CA will be detailed, in which the desired neural networks architectures among multiple datasets are optimized simultaneously.

A. Collaborative Analysis Framework

Traditional methods only achieve one CD task on each dataset at a time, which cannot effectively mine spectral knowledge among multiple datasets and lacking of knowledge sharing. HSI data captured by the same sensor are correlated and share similar features because they represent the radiance or reflectance of ground targets. Similar spectral features provide a more robust collaborative analysis environment.

Considering an HSI-CD dataset as $\mathbf{D} \in \mathbb{R}^{H \times W \times B}$, with the size of $H \times W$ and the B bands, a traditional single-task analysis model is shown as follows:

$$\mathbf{x} = \arg \min T(\mathbf{D}), \quad \text{s.t. } \mathbf{X} \in \Omega_i \quad (1)$$

where \mathbf{x} is an artificially designed network solution in the search space Ω_i and T represents the network learning of \mathbf{D} .

As shown in (1), the traditional model is limited to network training in one dataset. It means that once the dataset is changed, the learning of the network will be restarted. In order to avoid zero-basic learning when switching tasks and utilize the similarity between multiple HSI datasets more sufficiently, the cooperative analysis of multiple HSI images is proposed. The CA framework can transfer the positive information among optimization tasks, which can be stated as (2), which considers M datasets simultaneously

$$\begin{aligned} & \{\mathbf{x}_1, \mathbf{x}_2, \dots, \mathbf{x}_M\} \\ & = \arg \min \{T_1(\mathbf{D}_1), \dots, T_M(\mathbf{D}_M)\} \\ & \text{s.t. } \mathbf{D}_i \in \Omega_i, \quad i = 1, 2, \dots, M \end{aligned} \quad (2)$$

$$\begin{aligned} \min_{\theta_i} T_i(\mathbf{D}_i) &= \lambda_1 \|f(\mathbf{t}_x(\mathbf{D}_i); \theta_i) - \mathbf{t}_y(\mathbf{D}_i)\|_2 \\ &+ \lambda_2 L_p(\theta_i) \end{aligned} \quad (3)$$

where \mathbf{x}_i is a feasible solution, $\|f(\mathbf{t}_x(\mathbf{D}_i); \theta_i) - \mathbf{t}_y(\mathbf{D}_i)\|_2$ is the training loss, and $L_p(\theta_i)$ is the estimation of trainable parameters of i th network solution of task T_i , with θ_i the parameters of network. λ_1 and λ_2 represent the weight for each evaluation index. $\mathbf{t}_x(\mathbf{D}_i)$ and $\mathbf{t}_y(\mathbf{D}_i)$ are the training samples and labels of the i th dataset \mathbf{X}_i , respectively.

Compared with single dataset analysis, multiple dataset collaborative analysis can better explore the inherent correlation of similar tasks. The CA framework can facilitate the flow of information by cross-task sharing knowledge among tasks.

B. Self-Perception Network Architecture

In the traditional CD task, the network is fixed and generally designed in advance according to the prior knowledge of human experts. This fixed structure makes it feeble in the face of dataset switching and the process of network redesign is very monotonous and time-consuming. One of the effective solutions is establishing a self-adaptive network-designing method. In the cooperative analysis (CA) of multiple HSI images, all CD tasks are associated together to search for a better network structure for each task. Thus, in (2), $T_i(\mathbf{D}_i)$

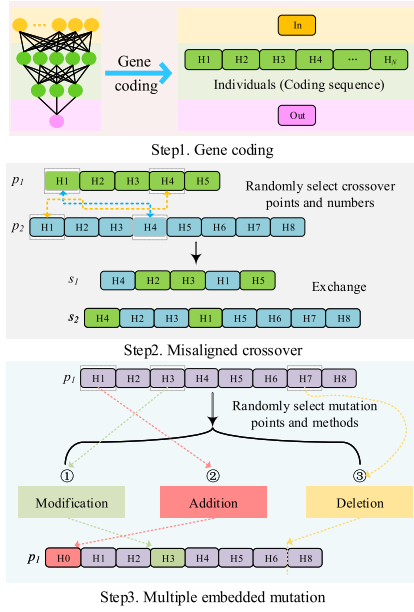


Fig. 2. Flowchart of genetic operation of SPNA.

is a self-perception network optimization task for dataset D_i . As shown in step.2 of Fig. 1, a population with fixed number (population size N_p) of individuals is used to construct an SPNA task. During the optimization process of SPNA tasks, genetic operation (crossover and mutation) is conducive to evolution with more diversity and is easier to produce promising architectures, as shown in Fig. 2.

1) *Gene Encoding*: In SPNA, gene encoding is applied to represent the indeterminate depth and the number of neurons in each hidden layer in neural networks.

2) *Crossover and Mutation Operator*: In Fig. 2, SPNA employs misaligned crossover to build offspring solution out of parameter values. Later, the offspring solutions were modified by a multiple embedded mutation operator to promote the diversity of the architectures.

3) *Fitness Evaluation*: The design of DNNs is required to consider multiple criteria (e.g., predictive performance and computational complexity). Theoretically, the individual with lower training error and computational complexity is preferred

$$F(x_i) = \lambda_1 L_t(x_i) + \lambda_2 L_p(x_i) \quad (4)$$

$$L_p(x_i) = \frac{P_{x_i}}{P_{\max}} \quad (5)$$

$$= \frac{n_1 + n_1^2 + n_1 * n_2 \cdots + n_{k-1} + n_{k-1} * n_k + n_k}{n_1 + n_m^2 + n_1 * n_m \cdots + n_m + n_m * n_K + n_K} \quad (6)$$

where $L_t(x_i)$ is the incomplete training loss of the network build with x_i , $L_p(x_i)$ is the parameter loss of the network, n_i is the neuron number of each layer, λ_1 and λ_2 represent weights for different evaluation index, which will be analyzed in Section III, P_{x_i} is the trainable parameter of current network, and P_{\max} is the trainable parameter of network with maximum neurons and layers.

4) *Hybrid-Criteria Evolution Strategy*: During the optimization of SPNA task, a hybrid-criteria evolution (HCE)

Algorithm 1 HCE Strategy

Input: Current population P_i , Population size N_p , Mating pool size N_{mp} , Discard probability P_D .
Output: Next population P_{i+1} .

```

1  $P_{i+1} \leftarrow \emptyset$ ;
2  $MP \leftarrow$  select best  $N_{mp}$  individuals of  $P_i$ ;
3  $P_{p+o} \leftarrow P_i$ ;
4 while  $MP \neq \emptyset$  do
5    $p_1, p_2 \leftarrow$  Randomly select parents from  $MP$ ;
6    $offspring \leftarrow$  Crossover & Mutation( $p_1, p_2$ );
7    $P_{p+o} \leftarrow$  Add  $offspring$  to right of  $P_{p+o}$ ; #Young
8 end
9  $o_1 \leftarrow$  The oldest individual of  $P_{p+o}$ ;
10  $o_2 \leftarrow$  The individual with the poorest fitness of  $P_{p+o}$ ;
11 while size of  $P_{p+o} > N_p$  do
12   if  $rand(0, 1) < P_D$  then
13      $P_{p+o} \leftarrow$  Remove  $o_1$  from left of  $P_{p+o}$ ; #Old
14   else
15      $P_{p+o} \leftarrow$  Remove  $o_2$  from  $P_{p+o}$ ;
16   end
17 end
18  $P_{i+1} \leftarrow P_{p+o}$ ;
19 return  $P_{i+1}$ .
```

strategy is proposed to select the elite individual for reproduction, considering the performance and the searching capacity. As shown in Algorithm 1, the individuals with poor performance and long-searching time will be discarded, which makes the joint search space of the multiple CD tasks more reasonable, instead of zooming in on good models too early.

C. Cross-Task Knowledge Transfer Mechanism

The optimization of SPNA-CA takes place in two ways. On the one hand, individuals from the same task can generate offspring through routine crossover and mutation operations (intratask evolution). On the other hand, the top-ranked individuals with promising fitness from different tasks can transfer according to the adaptive experience sharing probability P_{es} (cross-task communication). During the evolution of each task in Fig. 1, the top-ranked individuals with promising fitness are selected to transfer with adaptive experience sharing probability P_{es} , which leverages the migration effects of the current generation to dynamically guide the generation of next population

$$P_{es} = 1 - \min\{F(I)\} / \mu_m\{F(I)\} \quad (7)$$

where I represents all individuals of the population, $I = I_1, I_2, \dots, I_k$, k is the population size, and μ_m means the median of fitness for all individuals I . To be specific, if P_{es} becomes larger, which means that the knowledge transfer brings positive effects for the current generation; then, the next population should fully exploit the information of other tasks. Further analysis of P_{es} will be presented in Section III.

During each update of population, the encoded knowledge of excellent individuals is processed and shared across

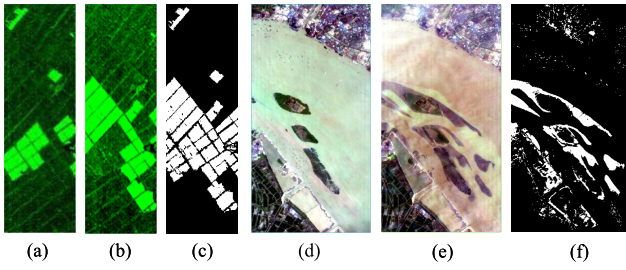


Fig. 3. Datasets. (a) Farm I_1 . (b) Farm I_2 . (c) Reference of Farm. (d) River I_1 . (e) River I_2 . (f) Reference of River.

TABLE I

EVALUATION INDEXES OF CD RESULTS

Data set	Method	PCC	Kappa
Farm	CVA	0.9528	0.8866
	DSFA	0.9534	0.8856
	GETNET	0.9637	0.9104
	SPNA-CA	0.9672	0.9200
River	CVA	0.9276	0.6601
	DSFA	0.9511	0.9478
	GETNET	0.9524	0.7333
	SPNA-CA	0.9548	0.6807

different SPNA tasks, where knowledge pertaining to different tasks is abstracted, stored, and reused for solving relevant problems whenever needed.

III. EXPERIMENTAL STUDY

In this section, experimental datasets and evaluation indices are briefly introduced at first. Then, the experimental performances of the proposed method and other state-of-the-art methods are analyzed in detail, in which visual results and evaluation indices are shown for theoretical analysis.

A. Experimental Datasets and Evaluation Indexes

As shown in Fig. 3, the first dataset “Farm” covers farmland near the city of Yancheng, Jiangsu province, China, with a size of 450×140 pixels and 155 bands selected after noise elimination. The second dataset “River” is acquired in Jiangsu province, China, which has a size of 463×241 pixels, with 198 bands available after noisy band removal.

Both of the two datasets are selected from Earth Observing-1 (EO-1) Hyperion images, which covers the $0.4\text{--}2.5\text{-}\mu\text{m}$ spectral range, with 242 spectral bands.

In our experiments, except the intuitively visual way of showing CD images, overall accuracy (OA), Kappa coefficients [11], first error measure (F_1 score), and the area under the receiver operating characteristics curves (AUC) [10] are used to evaluate the proposed method quantitatively.

B. Experimental Result

1) *CD Performance Analysis*: In the experiment, the CD results on Farm and River datasets are shown in Figs. 4 and 5, respectively, where different colors represent changed region (white) and unchanged region (black).

Fig. 4(a)–(d) shows the CD results achieved by CVA [9], DSFA [10], GETNET [11], and SPNA-CA (proposed), respectively. On the River dataset, DSFA and SPNA-CA (proposed)

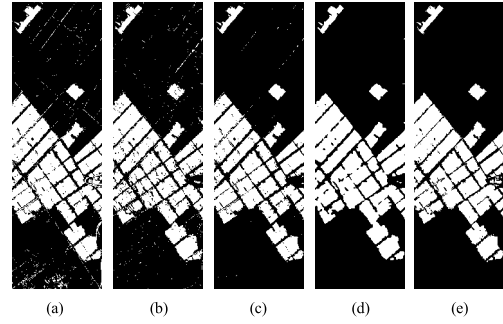


Fig. 4. CD results on Farm. (a) CVA. (b) DSFA. (c) GETNET. (d) SPNA-CA. (e) Reference.

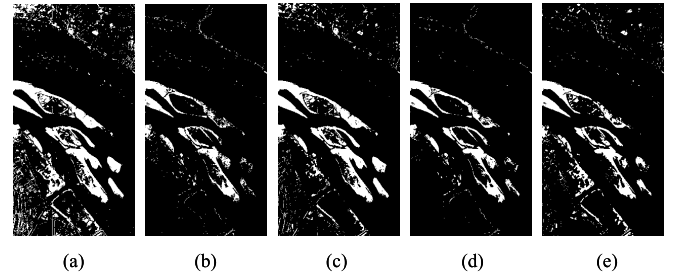


Fig. 5. CD results on River. (a) CVA. (b) DSFA. (c) GETNET. (d) SPNA-CA. (e) Reference.

TABLE II

NETWORK COMPLEXITY OF DIFFERENT METHODS

Data set	Method	Hidden layers	Parameters
River	DSFA	128(F)-128(F)	82,160
	GETNET	32(C)-64(C)-128(C)-96(C)-512(F)	154,178,998
	SPNA-CA	33(F)-14(F)-14(F)	46,745

have similarly good performances visually in unchanged areas, while SPNA-CA detects more changed areas than other methods. However, the CD results achieved by CVA and GETNET suffer from speckle noise and cause a lot of false detection, and CVA is particularly serious. As shown in Fig. 5(a)–(c), the CD result achieved by the proposed method suffers less speckle noise than others, and SPNA-CA presents more completely changed regions than the CVA, DSFA, and GETNET.

Table I shows the qualitative results of the compared methods, which indicates that SPNA-CA performs approximately best on both Farm and River datasets. Furthermore, the neural networks generated by SPNA-CA have simpler architecture and less parameters against other methods, while the DSFA uses two hidden layers and GETNET uses four convolutional layers and one fully connected layer. In Table II, “F” means the fully connected layer and “C” means the convolutional layer.

2) *Hyperparameter Analysis*: λ_1 and λ_2 are the weight for each evaluation index, where $\lambda_1 + \lambda_2 = 1$, in 5. In order to explore the proportional relationship, a series of experiments is carried out, which is shown in the relationship curves between CD performance and λ_2 in Fig. 6.

Since λ_2 is only an auxiliary coefficient, which is used to measure the computational complexity of the network, the experiment is only conducted for its value range of 0.1–0.5.

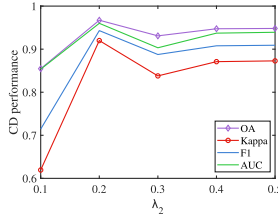


Fig. 6. CD Performance with different values of λ_2 .

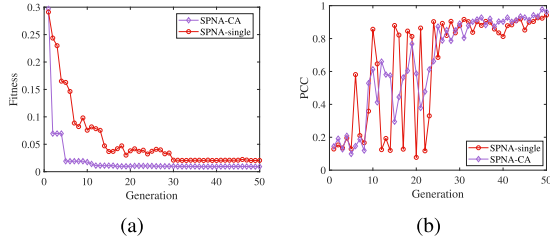


Fig. 7. Performance with collaborative SPNA-CA and single-task SPNA. (a) Fitness evaluation. (b) PCC evaluation.

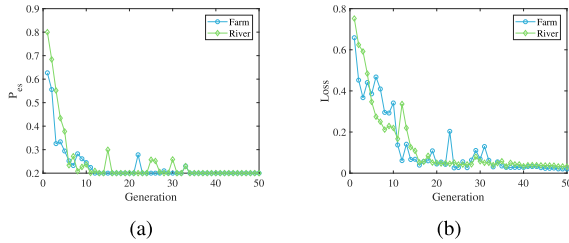


Fig. 8. Analysis of adaptive experience sharing probability P_{es} . (a) P_{es} changes during optimization. (b) Loss evaluation associated with P_{es} .

As a result, when $\lambda_2 = 0.2$, the network shows better CD performance than other circumstances.

3) *Analysis of Collaborative Analysis:* As shown in Fig. 7, faster convergence and higher accuracy are observed in collaborative SPNA-CA (two tasks) compared with two single-task SPNA. During iteration, the fluctuation of the SPNA-CA method is smaller, and the percent correct classification (PCC) values tend to stable state faster and finally obtain higher PCC value than the SPNA-single method.

As shown in Fig. 8(a), at the initial stage of the population, individuals within a population often dispersed greatly in fitness, so the P_{es} value is larger, which means that the communication between different tasks is more frequent. In the later stage of population optimization, the SPNA solutions of different datasets have been optimized to a certain extent, as shown in Fig. 8(b), which may pay more attention to its own task, so the value of P_{es} becomes smaller.

IV. CONCLUSION

HSI data obtained by the same sensor are correlated and share similar features because they represent the radiance or reflectance of ground targets. Traditional CD method based on

deep neural networks (DNNs) only deals with one dataset at a time, which has limited learning knowledge and undoubtedly fails to take advantage of the common characteristics among similar datasets. In this letter, an evolutionary multitasking method SPNA-CA is designed to facilitate the knowledge sharing of different network architecture searching tasks among multiple datasets to solve HSI-CD problems. More importantly, a CKTM is proposed to improve the cooperation ability of collaborative analysis framework and strengthen the searching efficiency.

Experimental results demonstrate the promising performances of the proposed method on solving HSI-CD problems. Besides, the subsequent results of exploring the effectiveness of CA suggest that the proposed method works more efficiently than other methods and successfully enhances accuracy and convergence compared to single dataset analysis.

REFERENCES

- [1] L. Bruzzone and S. B. Serpico, "An iterative technique for the detection of land-cover transitions in multitemporal remote-sensing images," *IEEE Trans. Geosci. Remote Sens.*, vol. 35, no. 4, pp. 858–867, Jul. 1997.
- [2] M. Gong, J. Zhao, J. Liu, Q. Miao, and L. Jiao, "Change detection in synthetic aperture radar images based on deep neural networks," *IEEE Trans. Neural Netw. Learn. Syst.*, vol. 27, no. 1, pp. 125–138, Jan. 2016.
- [3] S. Hu, L. Tong, A. E. Frazier, and Y. Liu, "Urban boundary extraction and sprawl analysis using landsat images: A case study in Wuhan, China," *Habitat Int.*, vol. 47, pp. 183–195, Jun. 2015.
- [4] P. Duan, P. Ghamisi, X. Kang, B. Rasti, S. Li, and R. Gloaguen, "Fusion of dual spatial information for hyperspectral image classification," *IEEE Trans. Geosci. Remote Sens.*, vol. 59, no. 8, pp. 7726–7738, Sep. 2020.
- [5] J. Ren, Z. Zabalza, S. Marshall, and J. Zheng, "Effective feature extraction and data reduction in remote sensing using hyperspectral imaging," *IEEE Signal Process. Mag.*, vol. 31, no. 4, pp. 149–154, Jul. 2014.
- [6] P. Duan, X. Kang, and S. Li, "Convolutional neural network for natural color visualization of hyperspectral images," in *Proc. IEEE Int. Geosci. Remote Sens. Symp. (IGARSS)*, Jul. 2019, pp. 3372–3375.
- [7] A. A. Nielsen, "The regularized iteratively reweighted mad method for change detection in multi- and hyperspectral data," *IEEE Trans. Image Process.*, vol. 16, no. 2, pp. 463–478, Feb. 2007.
- [8] V. Ortiz-Rivera, M. Velez-Reyes, and B. Roysam, "Change detection in hyperspectral imagery using temporal principal components," *Proc. SPIE*, vol. 6233, May 2006, Art. no. 623312.
- [9] F. Bovolo and L. Bruzzone, "A theoretical framework for unsupervised change detection based on change vector analysis in the polar domain," *IEEE Trans. Geosci. Remote Sens.*, vol. 45, no. 1, pp. 218–236, Jan. 2007.
- [10] B. Du, L. Ru, C. Wu, and L. Zhang, "Unsupervised deep slow feature analysis for change detection in multi-temporal remote sensing images," *IEEE Trans. Geosci. Remote Sens.*, vol. 57, no. 12, pp. 9976–9992, Dec. 2019.
- [11] Q. Wang, Z. Yuan, Q. Du, and X. Li, "GETNET: A general end-to-end 2-D CNN framework for hyperspectral image change detection," *IEEE Trans. Geosci. Remote Sens.*, vol. 57, no. 1, pp. 3–13, Jan. 2018.
- [12] S. Saha, L. Kondmann, Q. Song, and X. X. Zhu, "Change detection in hyperdimensional images using untrained models," *IEEE J. Sel. Topics Appl. Earth Observ. Remote Sens.*, vol. 14, pp. 11029–11041, 2021.
- [13] A. Erturk and G. Taskin, "Change detection with manifold embedding for hyperspectral images," in *Proc. 11th Workshop Hyperspectral Imag. Signal Process., Evol. Remote Sens. (WHISPERS)*, Mar. 2021, pp. 1–4.
- [14] S. Liu and Q. Shi, "Multitask deep learning with spectral knowledge for hyperspectral image classification," *IEEE Geosci. Remote Sens. Lett.*, vol. 17, no. 12, pp. 2110–2114, Dec. 2020.
- [15] D. Manolakis and G. S. Shaw, "Detection algorithms for hyperspectral imaging applications," *IEEE Signal Process. Mag.*, vol. 19, no. 1, pp. 29–43, Jan. 2002.
- [16] J. Shi, X. Liu, and Y. Lei, "SAR images change detection based on self-adaptive network architecture," *IEEE Geosci. Remote Sens. Lett.*, vol. 18, no. 7, pp. 1204–1208, Jul. 2021.